

# Monitoring statistics of the ERS-2 scatterometer for ESA

## cycle 95

(Project Ref. 18212/04/I-OL)

Hans Hersbach  
European Centre for Medium-Range Weather Forecasts,  
Shinfield Park, Reading, RG2 9AX, England  
Tel: (+44 118) 9499476, e-mail: dal@ecmwf.int

July 27, 2004

## 1 Introduction

On 21 August 2003, the world-wide dissemination of ERS-2 UWI data was restarted. Data is being recorded whenever within the visibility range of a ground station, leading for cycle 95 to a coverage of the North-Atlantic, part of the Mediterranean, the Gulf of Mexico, and to a small part of the Pacific north-west from the US and Canada (see Figure 2).

The quality of the UWI product was monitored at ECMWF for cycle 95. Results were compared to those obtained from the previous cycle, as well for data received during the nominal period in 2000 (up to cycle 59). No corrections for duplicate observations were applied.

During cycle 95, data was received between 21:06 UTC 17 May 2004 and 16:14 UTC 21 June 2004. Due to a cleaning procedure of the TWT (traveling Wave Tube), no data was received between 19:04 UTC 21 May 2004 and 13:44 UTC 25 May 2004. In general, largest volumes (typically 10,000) were received for 6-hourly data batches centered around 00 UTC; smallest amounts were recorded for the 06 UTC batches (around 700).

During cycle 95 the asymmetry between the fore and aft incidence angles developed a large positive bias. Around 18 June 2004 this bias exceeded 2.0 degrees, and since the asymmetry is one-to-one related to the yaw error, the combined  $k_p$ -yaw ESA flag was set for most observations. Around 12 UTC 18 June 2004, levels showed a sudden reduction, though were for the remainder of cycle 95 on average still positive. Besides this bias no real peaks were observed in the time series.

Compared to cycle 94, the agreement with ECMWF first-guess (FGAT) fields

has improved with regard to relative standard deviation (from 1.45 m/s to 1.39 m/s). This evolution is most probably related to seasonal variations of the non-global data coverage. Compared to cycle 94, the average relative bias was unchanged (-0.8 m/s), i.e., the UWI winds remain far too weak. The bias of the at ECMWF assimilated CMOD5 inverted winds has become more negative (from -0.28 m/s to -0.35 m/s). Although part of the bias fluctuations may originate from seasonal variations of the regional coverage, a similar though smaller negative trend was also observed for a global comparison between FGAT and QuikSCAT winds. A similar (smaller) global trend was for QuikSCAT also observed during 2003, but not for 2002. It is therefore difficult to state to what extent the developing relative bias of the UWI winds is to be attributed to changing instrument characteristics, or to changes in the wind climate.

Standard deviations are better than those for 2000; bias levels are comparable.

The quality of the UWI wind direction has slightly improved, while performance of de-aliased CMOD4 wind direction was nearly unchanged as compared to cycle 94.

The cycle-averaged evolution of performance relative to ECMWF FGAT winds is displayed in Figure 1. Figure 2 shows global maps of the over cycle 95 averaged UWI data coverage and wind climate, Figure 3 for performance relative to FGAT winds.

The ECMWF assimilation system was not changed during cycle 95.

## **2 ERS-2 statistics from 18 May to 21 June 2004**

### **2.1 Sigma0 bias levels**

The average sigma0 bias levels (compared to simulated sigma0's based on ECMWF model first-guess winds) stratified with respect to antenna beam, ascending or descending track and as function of incidence angle (i.e. across-node number) is displayed in Figure 4.

Compared to cycle 94, bias levels have for descending tracks become 0.15 dB more negative for all beams in a rather uniform way. For ascending tracks biases have for all beams grown by -0.1 dB in the mid and far range, and remained unchanged at low incidence angles.

Inter-node, inter-beam and inter-track bias variations are all within bounds; bias levels are in between -0.5 dB and -1.0 dB. Levels are about 0.15 dB more negative than for nominal data in 2000 (see Figure 1 of the reports for cycle 48 to 59).

The data volume of descending tracks is 23% lower than for ascending tracks.

### **2.2 Incidence angles**

For ESACA, across-node binning is, like the old processor, retained on a 25km mesh. From simple geometrical arguments it follows that variations in yaw attitude will lead to asymmetries between the incidence angles of the fore and aft beam. Indeed,

this has been observed. Figure 5 gives a time evolution of this asymmetry, showing rapid variations, which are typical for yaw attitude errors. Also in this figure, the occasions for which the combined  $k_p$ -yaw quality flag was set are indicated by red stars. The relation with incidence-angle asymmetries is obvious.

From Figure 5 it is seen that during cycle 95 there were no real anomalous periods. However, a considerable positive bias was developed, and well exceeded the 2-degree level around 16 June 2004. As a result, the  $k_p$ -yaw flag was set for most observations. Around 12 UTC 18 June 2004, however, the situation had suddenly improved, though a positive bias of approximately 1 degree did remain.

### 2.3 Distance to cone history

The distance to the cone history is shown in Figure 6. Curves are based on data that passed all QC, including the test on the  $k_p$ -yaw flag, however subject to the land and sea-ice check at ECMWF (see cyclic report 88 for details).

Like for cycle 94, time series are (due to lack of statistics) very noisy, especially for the first nodes. This makes it difficult to identify peaks that might indicate a low data quality. Most spikes are a result from low data volumes (such as for 17 to 19 June 2004).

Compared to cycle 94, the average level is slightly higher, from 1.20 to 1.24, and is now about 14% higher than for nominal data (see top panel Figure 1).

### 2.4 UWI minus First-Guess wind history

In Figure 7, the UWI minus ECMWF first-guess wind-speed history is plotted.

The history plot shows several peaks, most of which are related to low data volumes. Examples are 06 UTC 2 June, 06 UTC 12 June, 06 UTC 15 June and 18 UTC 16 June 2004.

Similar results apply for the history of de-aliased CMOD4 winds versus FGAT (Figure 9).

Figure 11 displays the locations for which UWI winds were more than 8 m/s weaker (top panel) and more than 8 m/s stronger (lower panel) than FGAT winds. The number of such collocations is low, and occur less frequent than for previous cycles. This could well be the result of a quieter wind climate. Two examples from such situations are given in Figure 12. The top panel (13:20 UTC 26 May 2004, Atlantic) shows an area of large disagreement between UWI and FGAT winds in a complex flow. The lower panel of Figure 12 (south of New Orleans) shows a patch of strong winds not present in the ECMWF model field.

Average bias levels and standard deviations of UWI winds relative to FGAT winds are displayed in Table 1. From this it is seen that the bias of both the UWI and CMOD4 product were unchanged (-0.80 m/s respectively -0.79 m/s). Biases are most negative in the near range (-1.29 m/s, was -1.40 m/s, see also third panel of Figure 1). The average bias level is comparable to that for nominal data in 2000 (UWI: -0.80 m/s now, was -0.79 m/s for cycle 59). The evolution of this bias between cycles 92 and 95 is displayed in the top panel of Figure 17. Here the red curve is

	cycle 94		cycle 95	
	UWI	CMOD4	UWI	CMOD4
speed STDV	1.45	1.44	1.39	1.39
node 1-2	1.45	1.43	1.41	1.41
node 3-4	1.39	1.38	1.37	1.37
node 5-7	1.37	1.37	1.34	1.34
node 8-10	1.39	1.39	1.34	1.34
node 11-14	1.41	1.41	1.37	1.38
node 15-19	1.47	1.47	1.40	1.40
speed BIAS	-0.80	-0.79	-0.80	-0.79
node 1-2	-1.40	-1.38	-1.29	-1.27
node 3-4	-1.10	-1.06	-1.05	-1.01
node 5-7	-0.84	-0.82	-0.83	-0.80
node 8-10	-0.62	-0.62	-0.66	-0.65
node 11-14	-0.58	-0.59	-0.61	-0.62
node 15-19	-0.58	-0.60	-0.63	-0.65
direction STDV	28.9	18.6	27.0	18.9
direction BIAS	-3.0	-3.2	-3.5	-3.5

Table 1: Biases and standard deviation of ERS-2 versus ECMWF FGAT winds in m/s for speed and degrees for direction

the 5-day moving average for the at ECMWF inverted ERS-2 winds; i.e., CMOD4 plus bias corrections before 9 March 2004 (blue vertical dashed line), and CMOD5 afterwards. A similar trend, though smaller, is also, though to a smaller extent, visible in the global statistics of QuikSCAT winds (middle panel). A similar trend for QuikSCAT data was observed during 2003, but not during 2002 (lower panel of Figure 17).

The standard deviation of UWI winds compared to cycle 94 has improved (1.39 m/s, was 1.45 m/s). Largest improvement was found at the highest incidence angles, making the inter-node performance more homogenous.

For cycle 95 the (UWI - FGAT) direction standard deviations were ranging between 15 and 40 degrees (Figure 8). Sharp peaks are the result of low data volumes. For de-aliased CMOD4 winds values between 20 and 30 degrees are most common (Figure 10).

With respect to cycle 94, the average standard deviation (see Table 1) of the UWI wind direction has slightly decreased (27.0 degrees, was 28.9 degrees). The performance of de-aliased CMOD4 winds was almost unchanged (18.9 degrees, was 18.6 degrees). Bias levels in wind direction became slightly more negative (-3.5 degrees, was -3.0 degrees for UWI; -3.5 degrees, was -3.2 degrees for de-aliased CMOD4).

## 2.5 Scatterplots

Scatterplots of FGAT winds versus ERS-2 winds are displayed in Figures 13 to 16. Values of standard deviations and biases are slightly different from those displayed in Table 1. Reason for this is that, for plotting purposes, the in 0.5 m/s resolution ERS-2 winds have been slightly perturbed (increases scatter with 0.02 m/s), and that zero wind-speed ERS-2 winds have been excluded (decreases scatter with about 0.05 m/s).

The scatterplot of UWI wind speed versus FGAT (Figure 13) is very similar to that for (at ECMWF inverted) de-aliased CMOD4 winds (Figure 15). It confirms that the ESACA inversion scheme is working properly. The reduced standard deviation compared to cycle 94 (1.41 m/s, was 1.46 m/s), originates from a less intense wind climate.

Winds derived on the basis of CMOD5 are displayed in Figure 16. The bias compared to FGAT winds is reasonably small for all wind domains though has grown into negative values over the last few cycles (on average -0.35 m/s, was -0.28 m/s for cycle 94). The relative standard deviation is lower than for CMOD4 winds (1.39 m/s versus 1.41 m/s).

## Figure Captions

**Figure 1:** Evolution of the performance of the ERS-2 scatterometer averaged over 5-weekly cycles from 12 December 2001 (cycle 69) to 21 June 2004 (end cycle 95) for the UWI product (solid, star) and de-aliased winds based on CMOD4 (dashed, diamond). Results are based on data that passed the UWI QC flags. For cycle 85 two values are plotted; the first value for the global set, the second one for the regional set. Dotted lines represent values for cycle 59 (5 December 2000 to 17 January 2001), i.e. the last stable cycle of the nominal period. From top to bottom panel are shown the normalized distance to the cone (CMOD4 only) the standard deviation of the wind speed compared to FGAT winds, the corresponding bias (for UWI winds the extreme inter-node averages are shown as well), and the standard deviation of wind direction compared to FGAT.

**Figure 2:** Average number of observations per 12H and per 125km grid box (top panel) and wind-climate (lower panel) for UWI winds that passed the UWI flags QC and a check on the collocated ECMWF land and sea-ice mask.

**Figure 3:** The same as Figure 2, but now for the relative bias (top panel) and standard deviation (lower panel) with ECMWF first-guess winds.

**Figure 4:** Ratio of  $\langle \sigma_0^{0.625} \rangle / \langle \text{CMOD4}(\text{FirstGuess})^{0.625} \rangle$  converted in dB for the fore beam (solid line), mid beam (dashed line) and aft beam (dotted line), as a function of incidence angle for descending and ascending tracks. The thin lines indicate the error bars on the estimated mean. First-guess winds are based on the in time closest (+3h, +6h, +9h, or +12h) T511 forecast field, and are bilinearly interpolated in space.

**Figure 5:** Time series of the difference in incidence angle between the fore and

aft beam. Red stars indicate the occurrences for which the combined  $k_p$ -yaw flag was set.

**Figure 6:** Mean normalized distance to the cone computed every 6 hours for nodes 1-2, 3-4, 5-7, 8-10, 11-14 and 15-19 (solid curve close to 1 when no instrumental problems are present). The dotted curve shows the number of incoming triplets in logarithmic scale (1 corresponds to 60,000 triplets) and the dashed one indicates the fraction of complete (based on the land and sea-ice mask at ECMWF) sea-located triplets rejected by ESA flags, or by the wind inversion algorithm (0: all data kept, 1: no data kept).

**Figure 7:** Mean (solid line) and standard deviation (dashed line) of the wind speed difference UWI - first guess for the data retained by the quality control.

**Figure 8:** Same as Fig. 7, but for the wind direction difference. Statistics are computed only for wind speeds higher than 4 m/s.

**Figures 9 and 10:** Same as Fig. 7 and 8 respectively, but for the de-aliased CMOD4 data.

**Figure 11:** Locations of data during cycle 95 for which UWI winds are more than 8 m/s weaker (top panel) respectively stronger (lower panel) than FGAT, and on which QC on UWI flags and the ECMWF land/sea-ice mask was applied.

**Figure 12:** Comparison between UWI (red) and ECMWF FGAT (blue) winds for a case on 26 May 2004 (top panel) and 27 May 2004 (lower panel).

**Figure 13:** Two-dimensional histogram of first guess and UWI wind speeds, for the data kept by the UWI flags, and QC based on the ECMWF ice and land and sea-ice mask. Circles denote the mean values in the y-direction, and squares those in the x-direction.

**Figure 14:** Same as Fig. 13, but for wind direction. Only wind speeds higher than 4m/s are taken into account.

**Figure 15:** Same as Fig. 13, but for de-aliased CMOD4 winds.

**Figure 16:** Same as Fig. 13, but for de-aliased CMOD5 winds.

**Figure 17:** Bias relative to FGAT winds of the wind speed of ERS-2 winds (based on bias-corrected CMOD4 before 9 March 2004, and on CMOD5 afterwards) for nodes 8-10 (top panel) respectively of 50-km QuikSCAT (based on the QSCAT-1 model function) for nodes 30-34 (middle and lower panels) versus ECMWF first guess for the period of cycle 92 to 95 (3 February 2004 to 21 June 2004). Curves represent centered 5-day running means for the top and middle panel, and a 30-day mean for the lower panel. Vertical dashed blue lines mark ECMWF model changes.

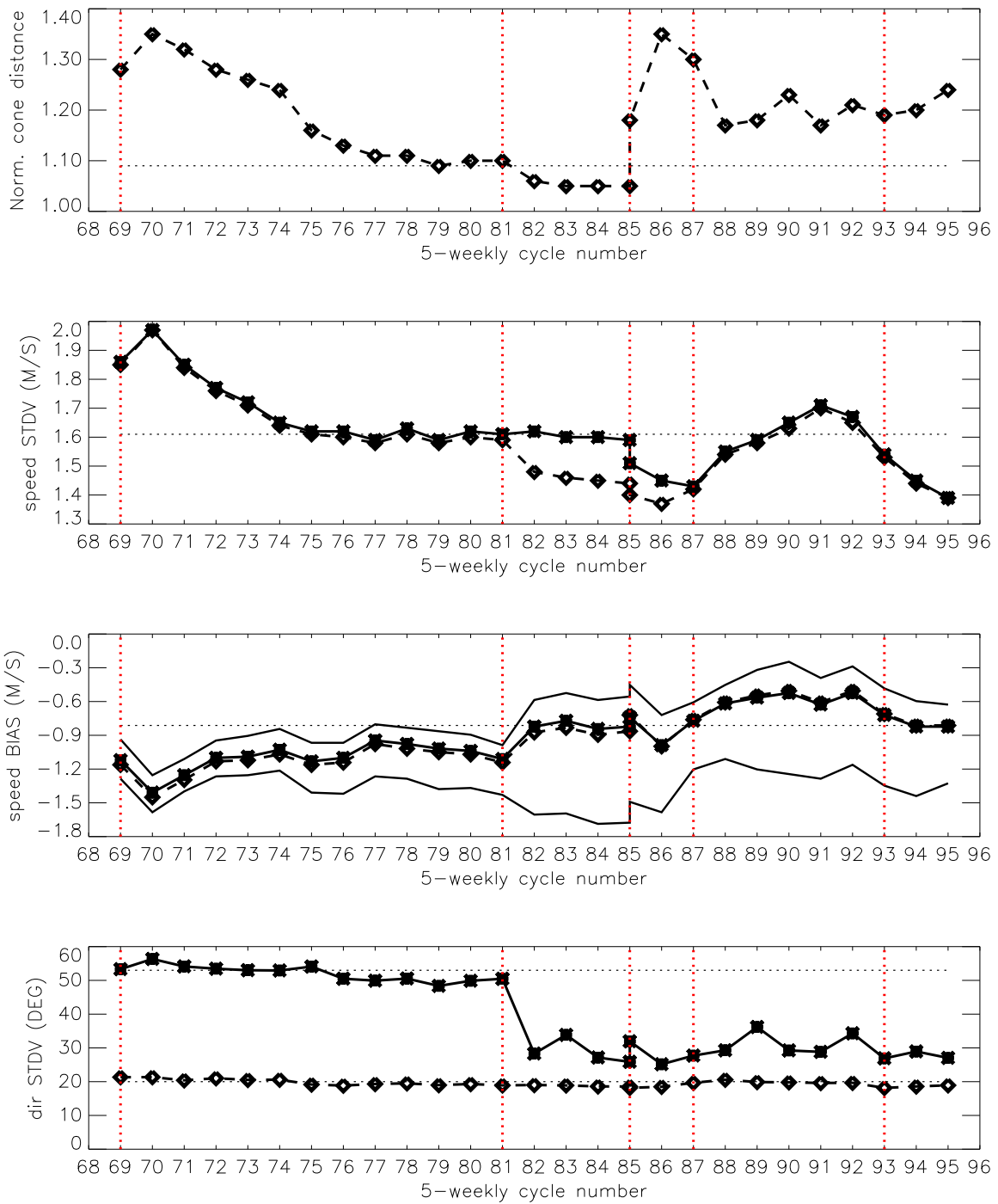
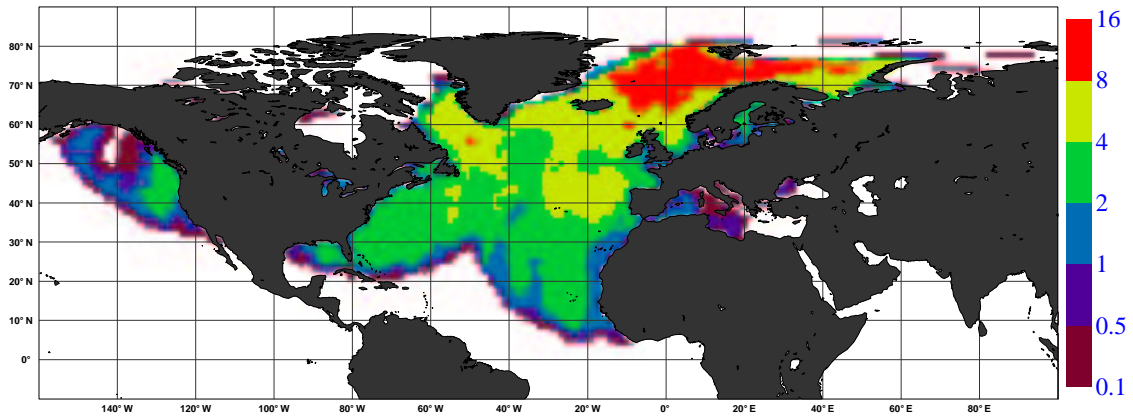


Figure 1

NOBS ( ERS-2 UWI ), per 12H, per 125km box  
average from 2004051800 to 2004062118 GLOB:2.898



AVERAGE ( ERS-2 UWI ), in m/s.  
average from 2004051800 to 2004062118 GLOB:5.505

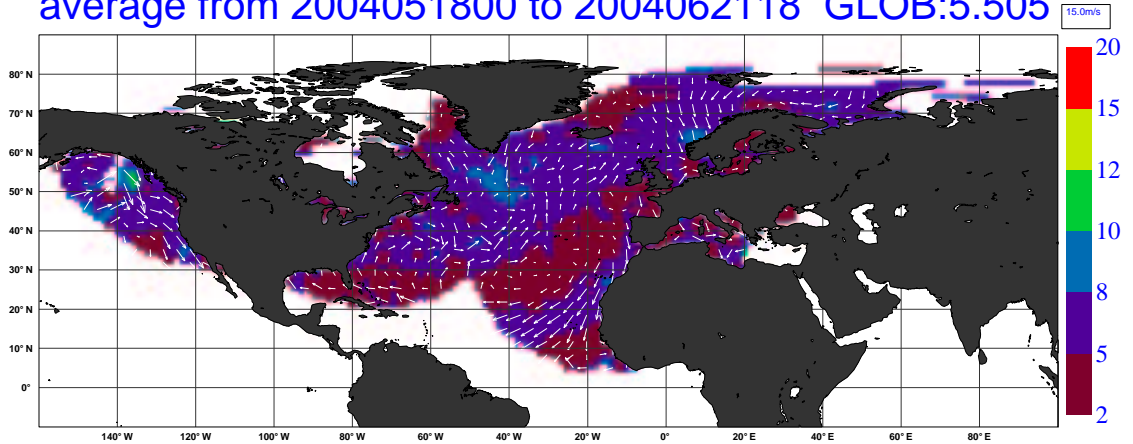
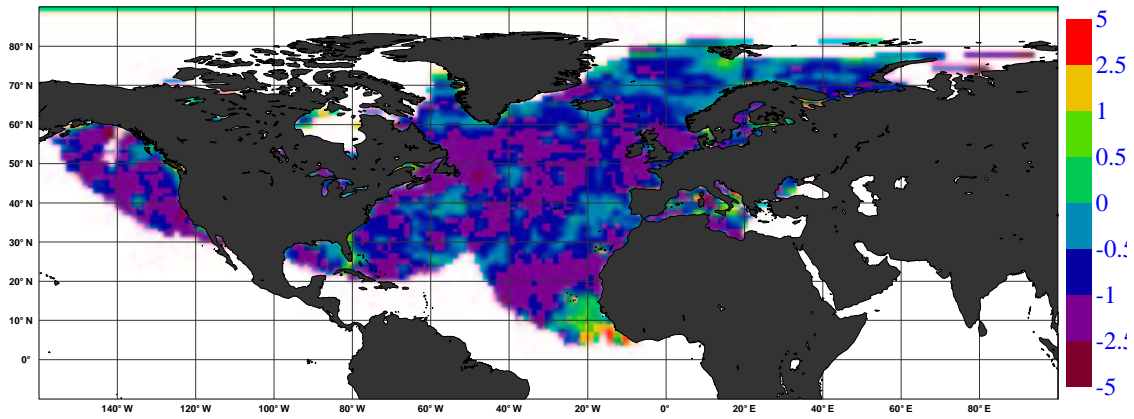


Figure 2

BIAS ( ERS-2 UWI vs FIRST-GUESS ), in m/s.  
average from 2004051800 to 2004062118 GLOB:-0.79



STDV ( ERS-2 UWI vs FIRST-GUESS ), in m/s.  
average from 2004051800 to 2004062118 GLOB:1.218

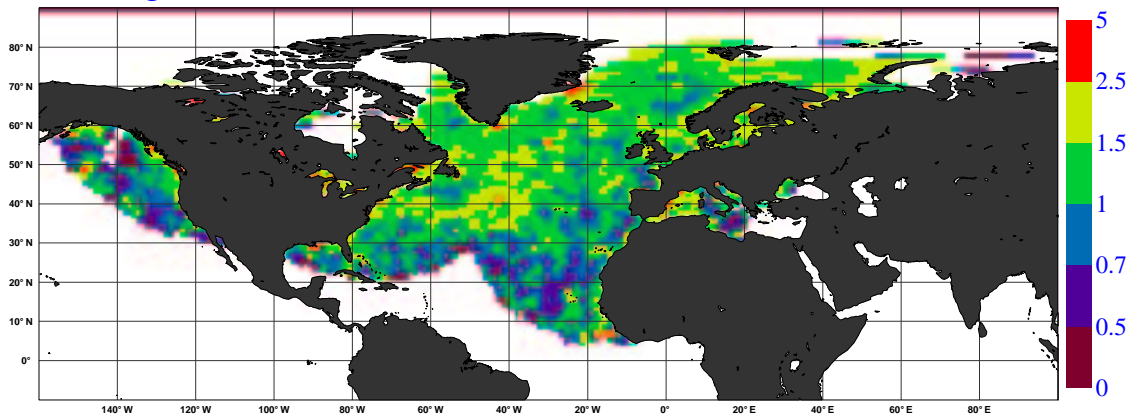


Figure 3

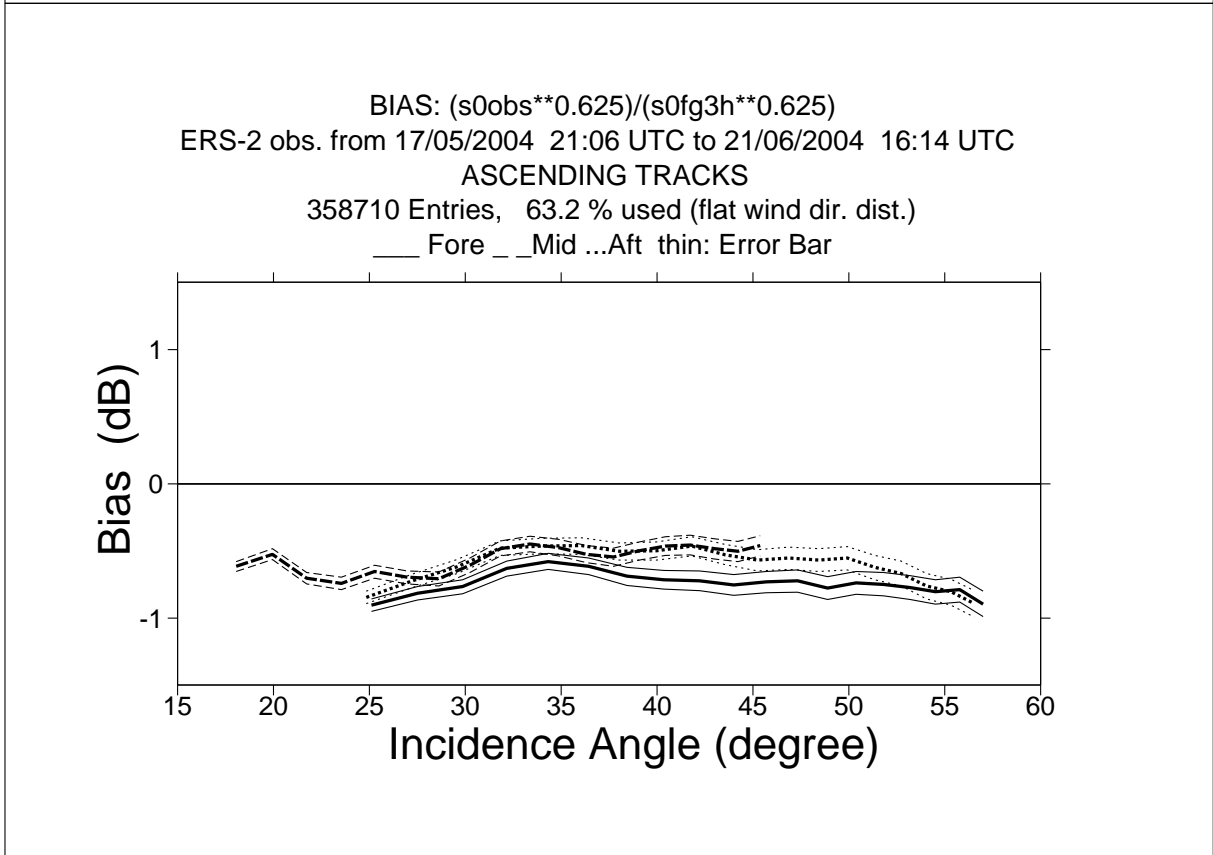
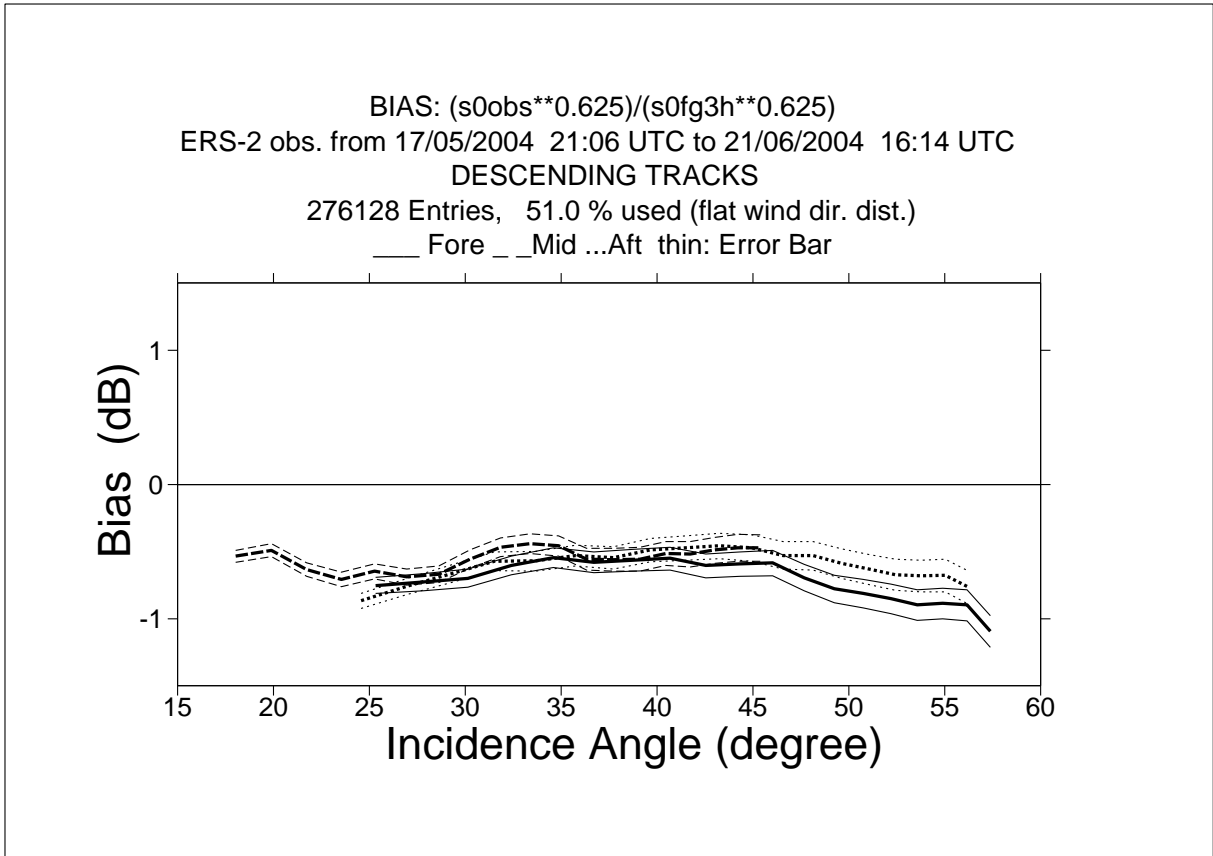


Figure 4



# Monitoring of Sigma0 triplets versus CMOD4 for ERS-2

from 2004051800 to 2004062118

(solid) mean normalised distance to the cone over 6 h

(dashed) fraction of complete sea-point observations rejected by ESA flag or CMOD4 inversion

(dotted) total number of data in log. scale (1 for 60000)

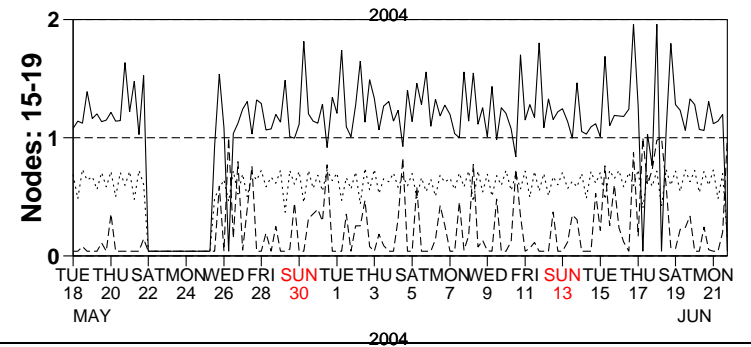
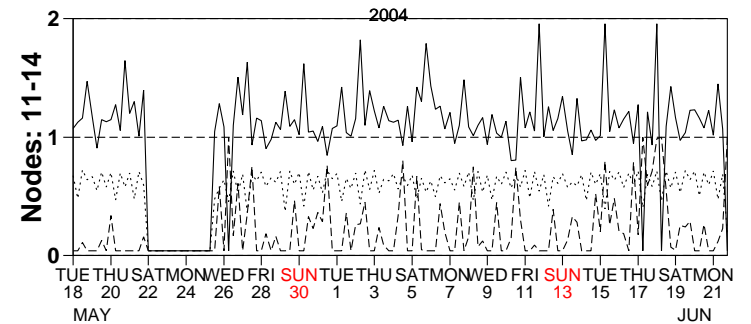
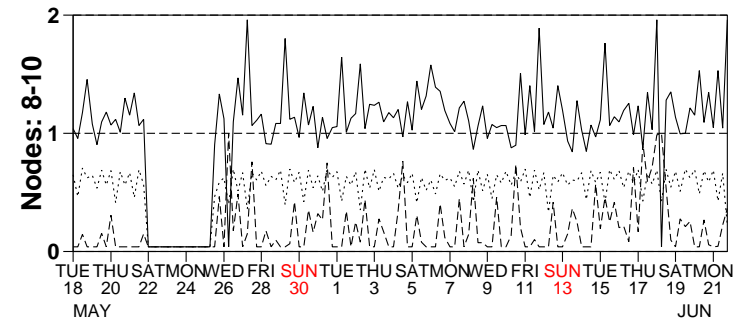
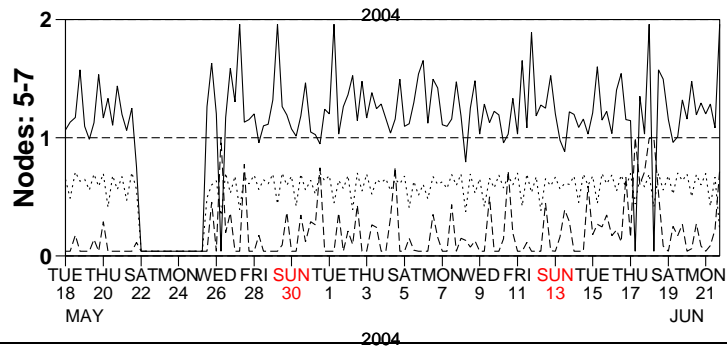
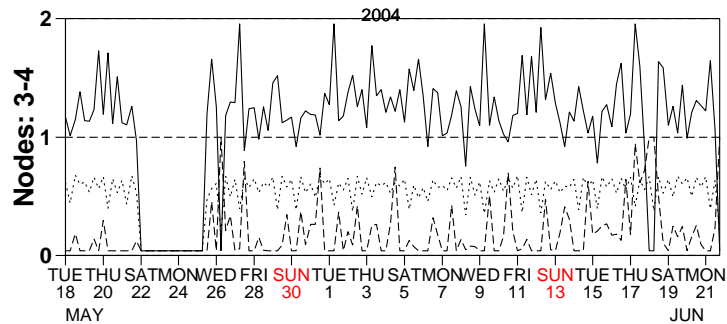
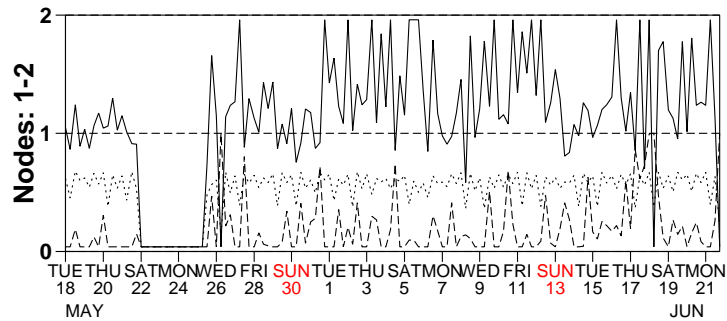


Figure 6

# Monitoring of UWI winds versus First Guess for ERS-2

from 2004051800 to 2004062118

(solid) wind speed bias UWI - First Guess over 6h (deg.)

(dashed) wind speed standard deviation UWI - First Guess over 6h (deg.)

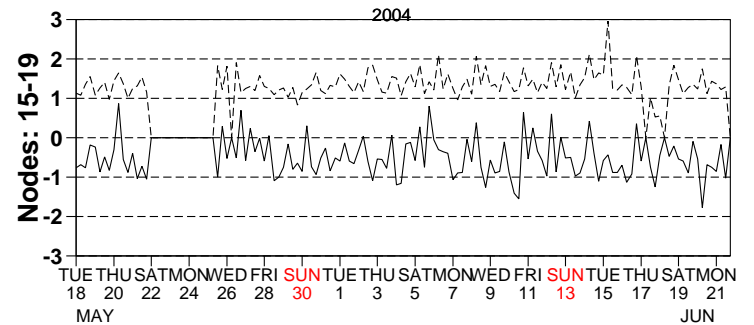
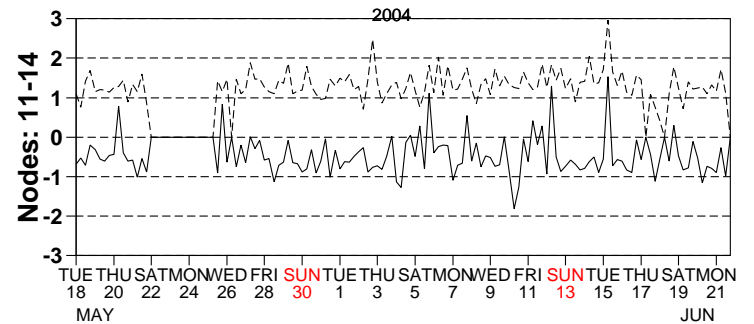
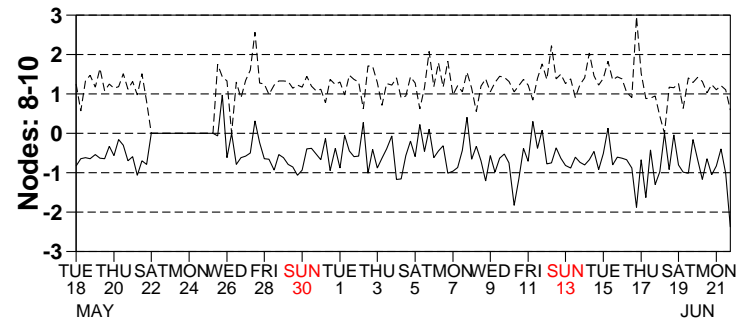
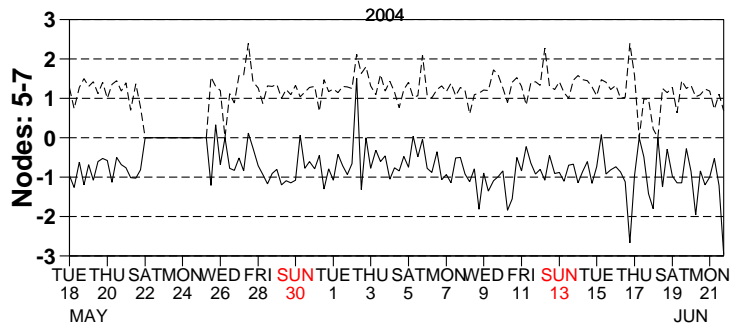
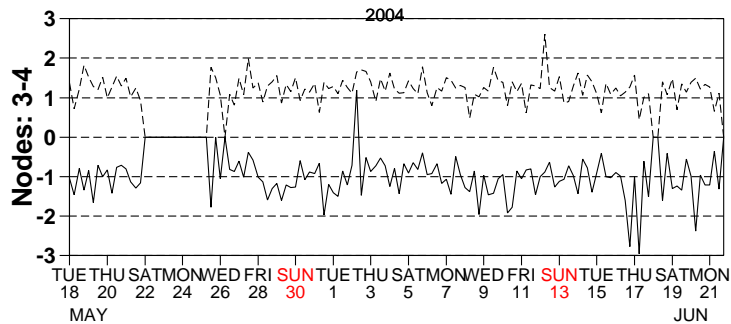
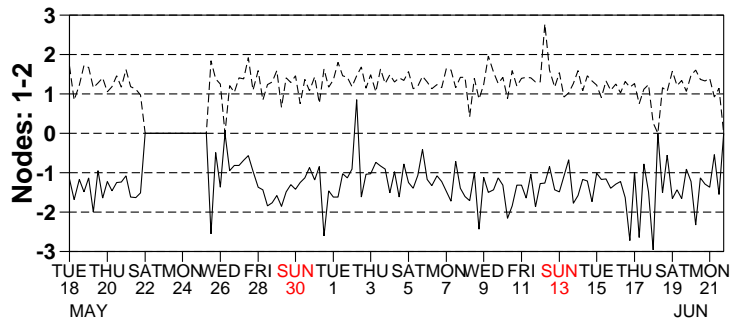


Figure 7

# Monitoring of UWI winds versus First Guess for ERS-2

from 2004051800 to 2004062118

(solid) wind direction bias UWI - First Guess over 6h (deg.)

(dashed) wind direction standard deviation UWI - First Guess over 6h (deg.)

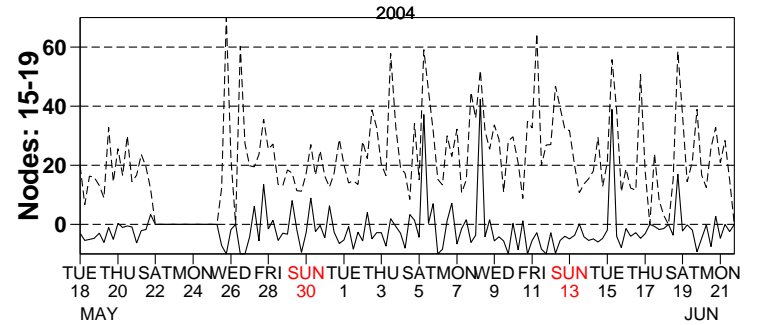
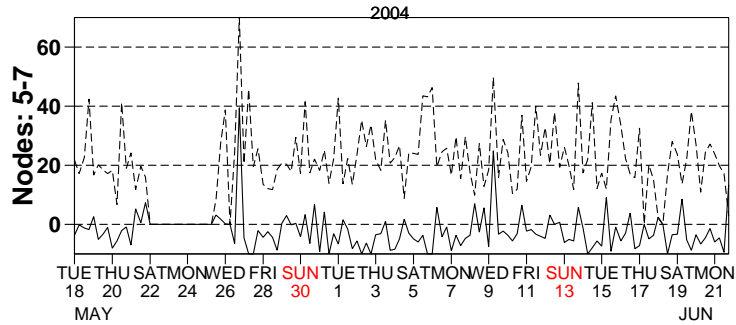
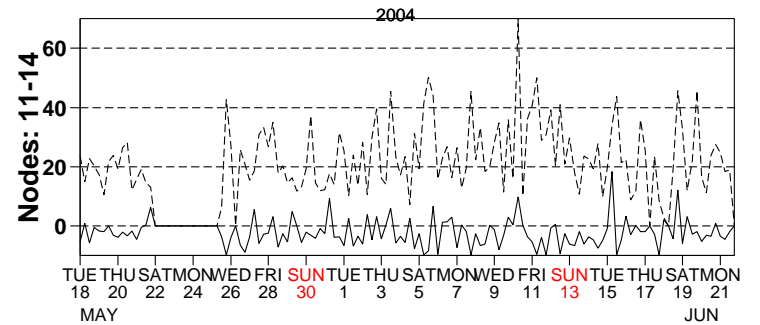
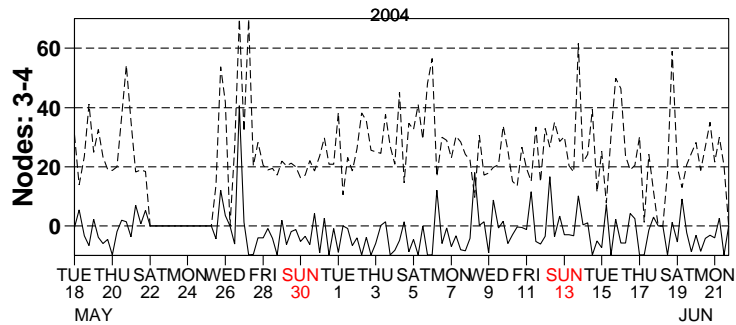
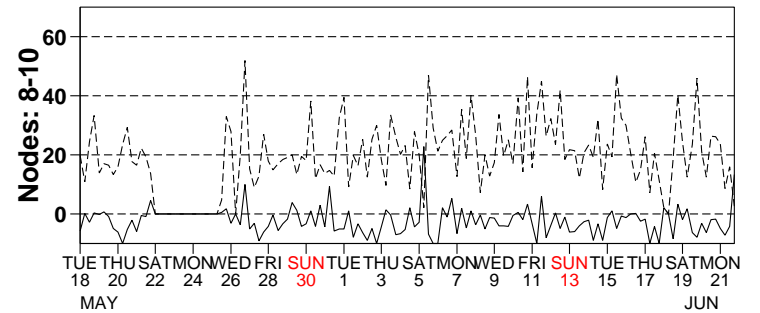
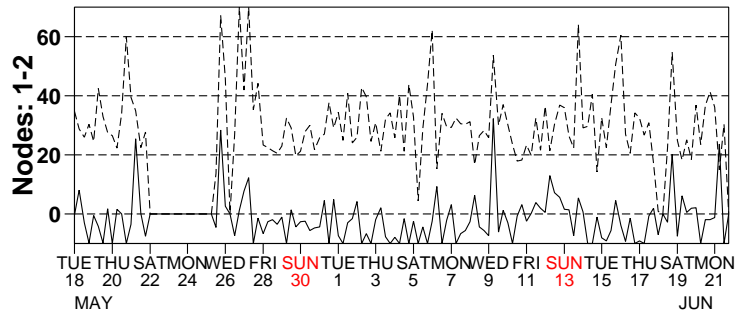


Figure 8

# Monitoring of de-aliased CMOD4 winds versus First Guess for ERS-2

from 2004051800 to 2004062118

(solid) wind speed bias CMOD4 - First Guess over 6h (deg.)

(dashed) wind speed standard deviation CMOD4 - First Guess over 6h (deg.)

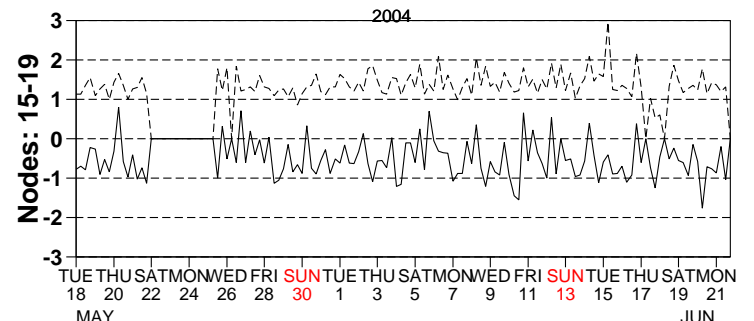
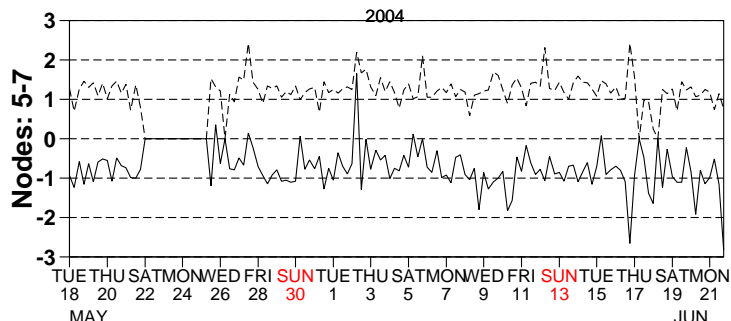
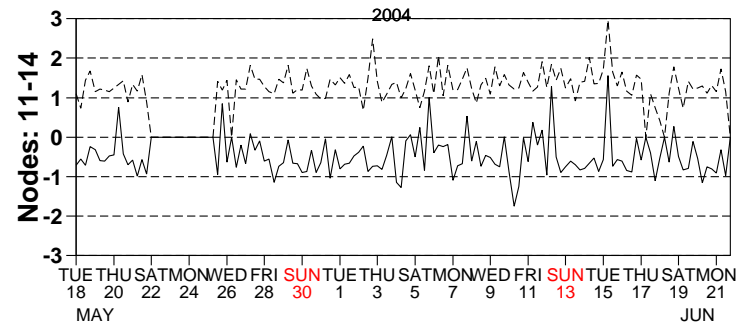
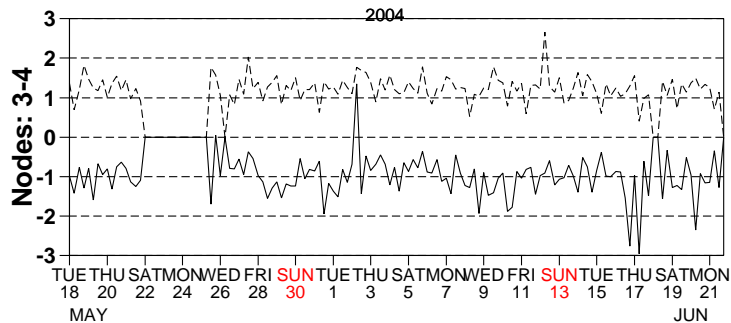
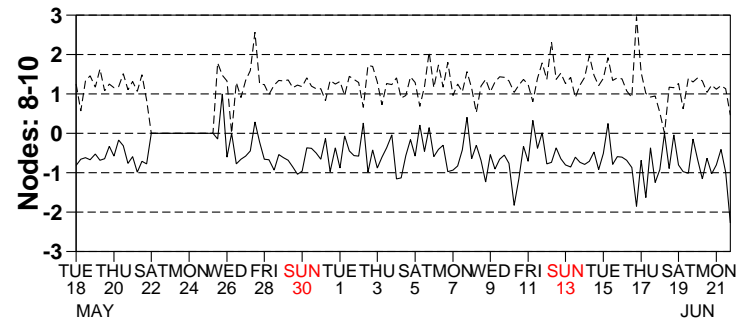
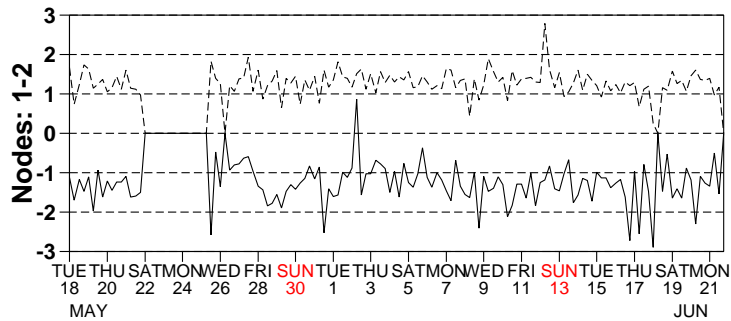


Figure 9

# Monitoring of de-aliased CMOD4 winds versus First Guess for ERS-2

from 2004051800 to 2004062118

(solid) wind direction bias CMOD4 - First Guess over 6h (deg.)

(dashed) wind direction standard deviation CMOD4 - First Guess over 6h (deg.)

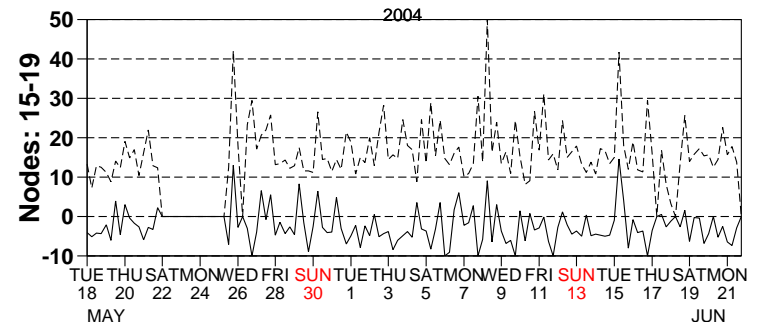
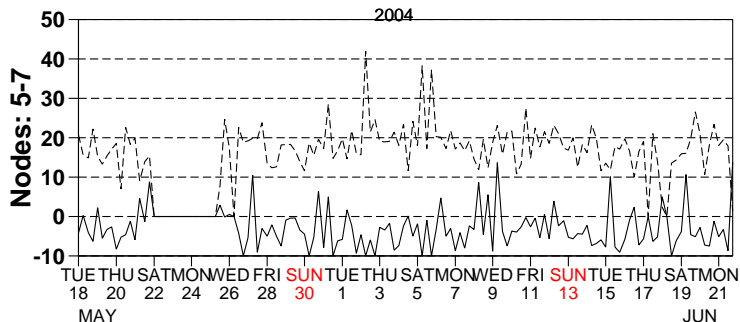
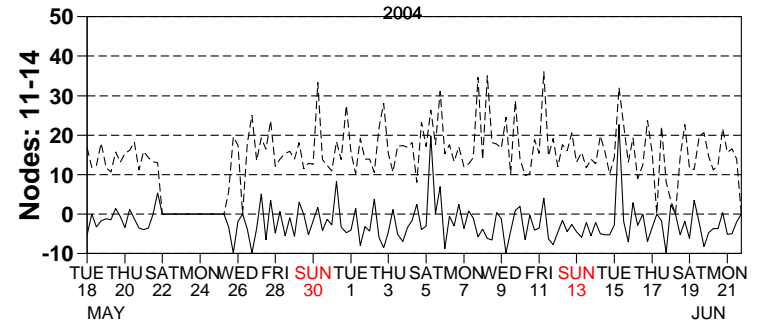
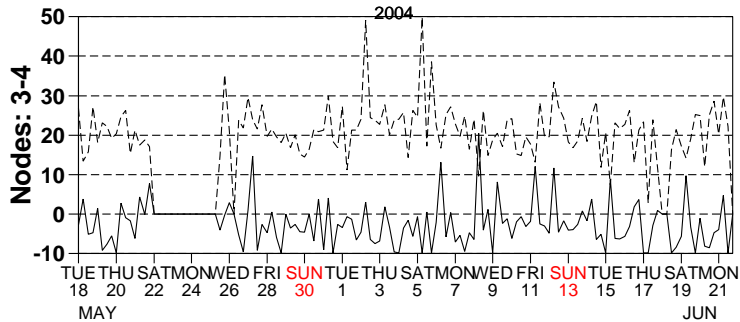
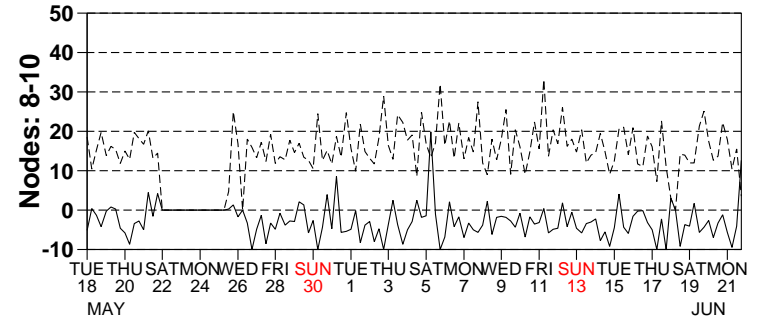
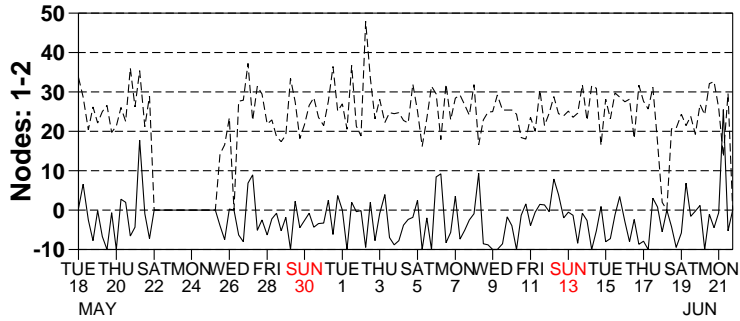
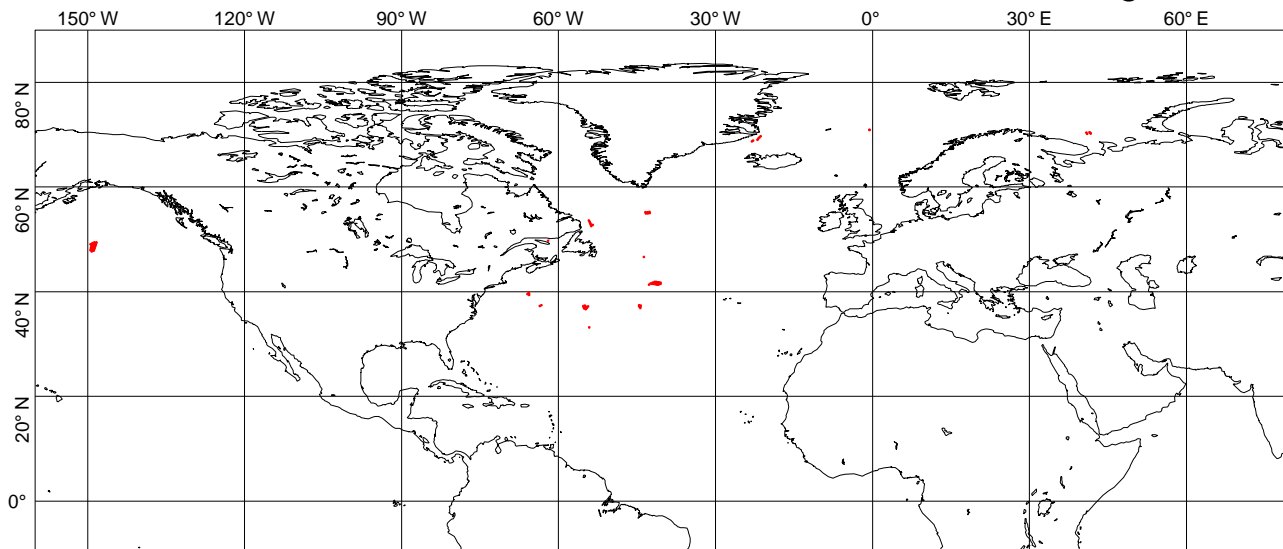


Figure 10

UWI winds more than 8 m/s weaker than FGAT  
CYCLE 95, 2004051800 to 2004062118, QC on ESA flags



UWI winds more than 8 m/s stronger than FGAT  
CYCLE 95, 2004051800 to 2004062118, QC on ESA flags

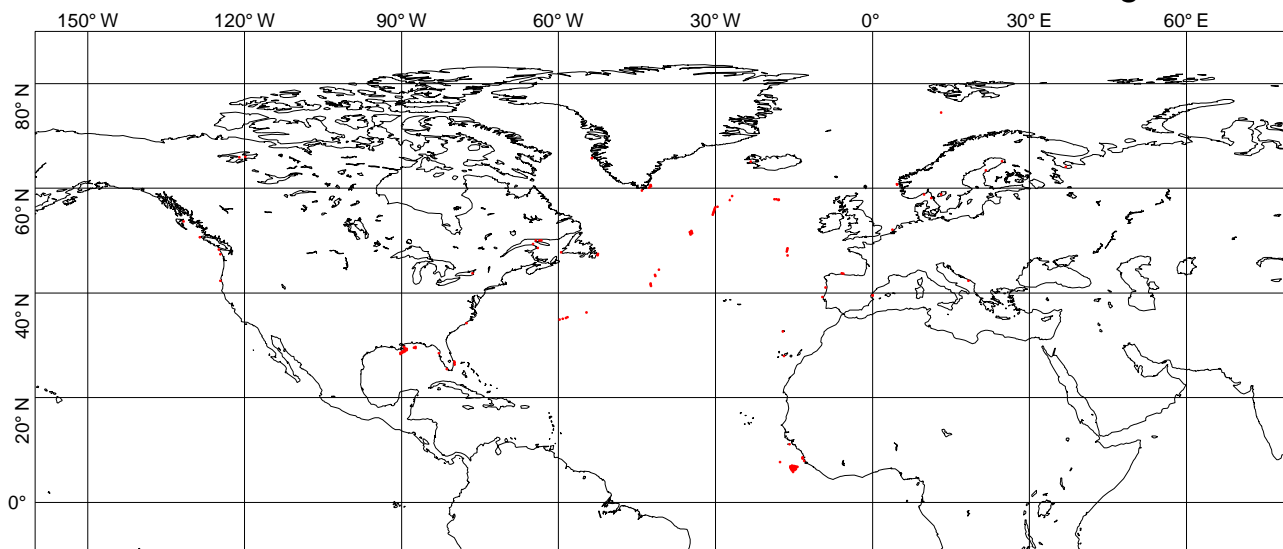
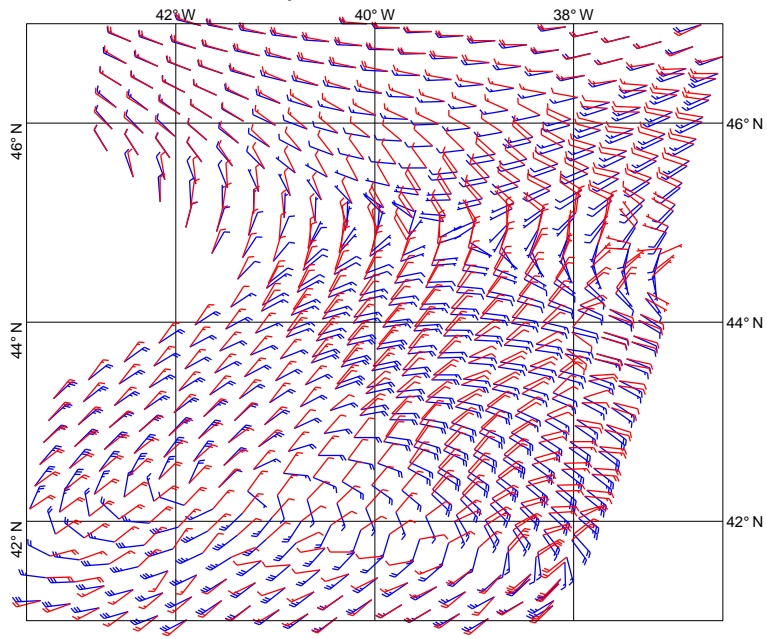


Figure 11

UWI winds (red) versus FGAT winds (blue)  
26 May 2004, 13:20 UTC



UWI winds (red) versus FGAT winds (blue)  
27 May 2004, 11:17 UTC

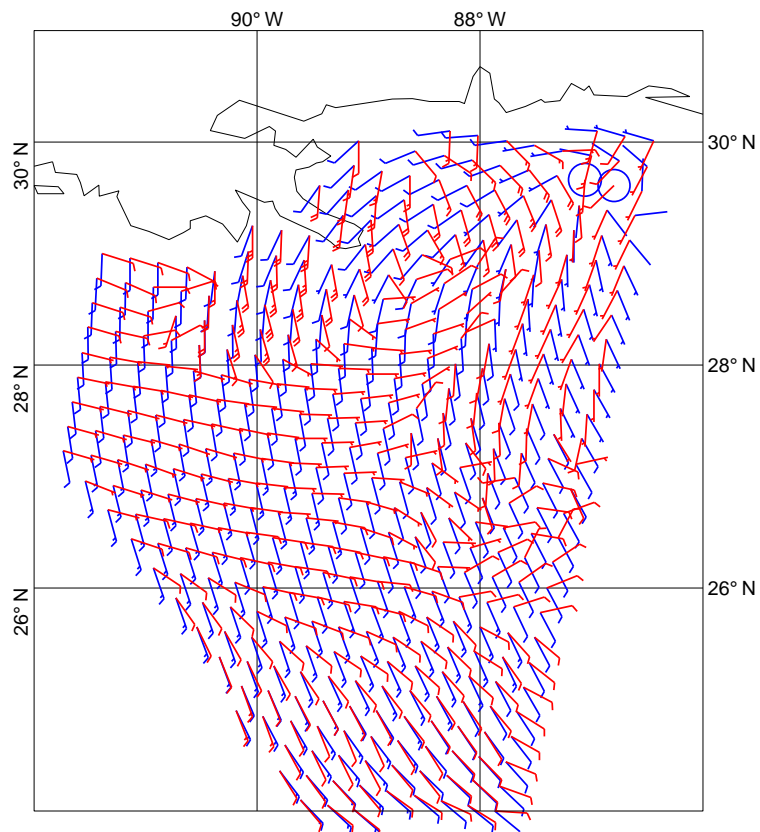


Figure 12

histogram of first guess 10 m winds versus uwi winds  
from 2004051800 to 2004030818  
= 634838, db contour levels, 5 db step, 1st level at 3.0 db  
 $m(y-x) = -0.80$   $sd(y-x) = 1.41$   $sdx = 3.04$   $sd y = 2.76$   $pcxy = 0.941$

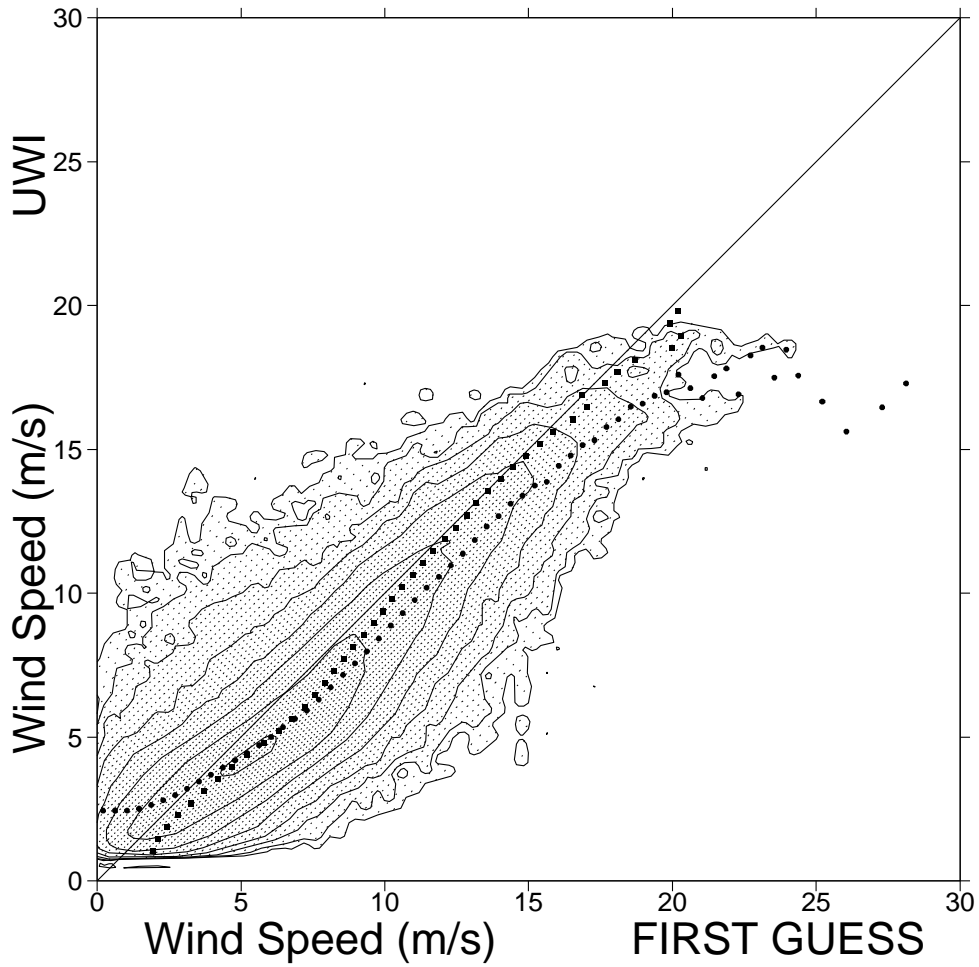


Figure 13

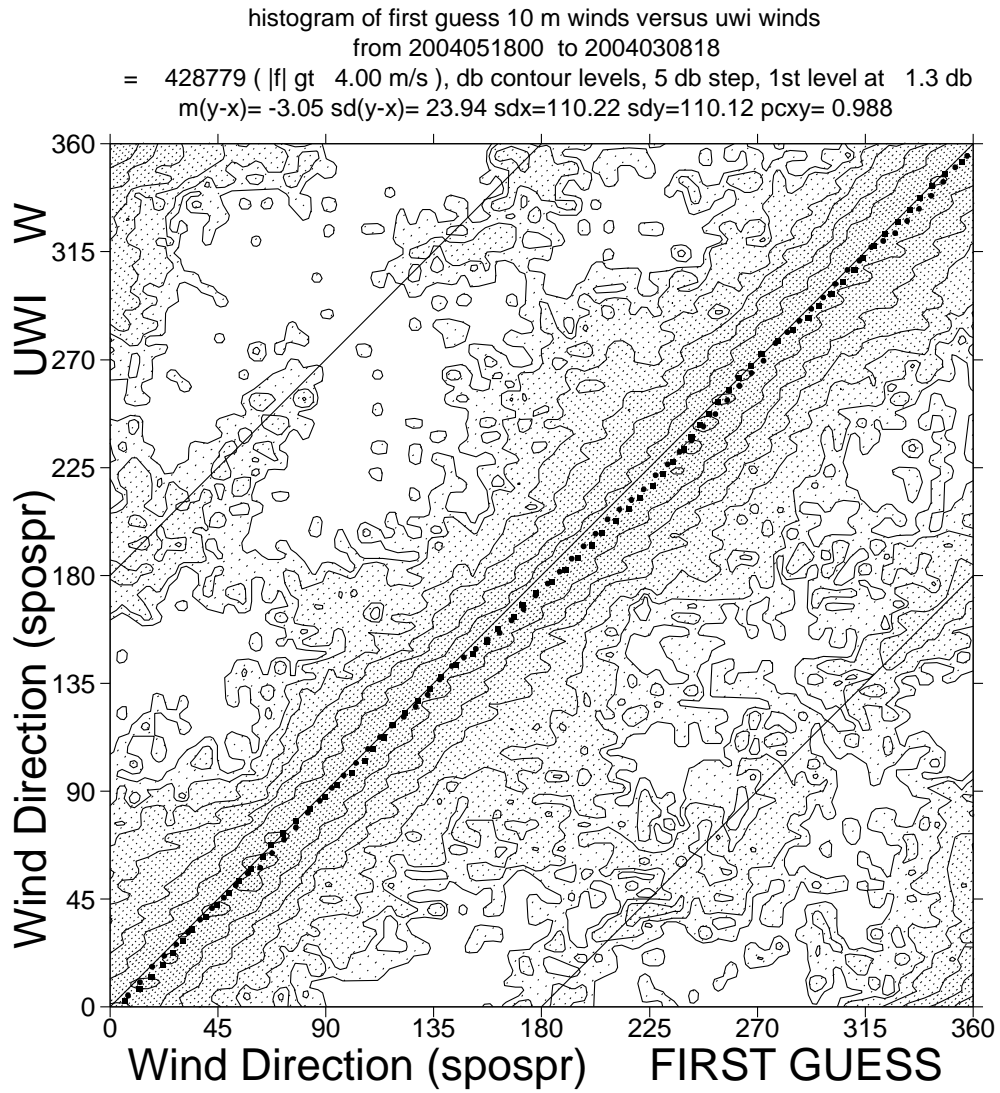


Figure 14

histogram of first guess 10 m winds versus uwi winds  
from 2004051800 to 2004030818  
= 633785, db contour levels, 5 db step, 1st level at 3.0 db  
 $m(y-x) = -0.79$   $sd(y-x) = 1.41$   $sdx = 3.04$   $sd_y = 2.75$   $pcxy = 0.941$

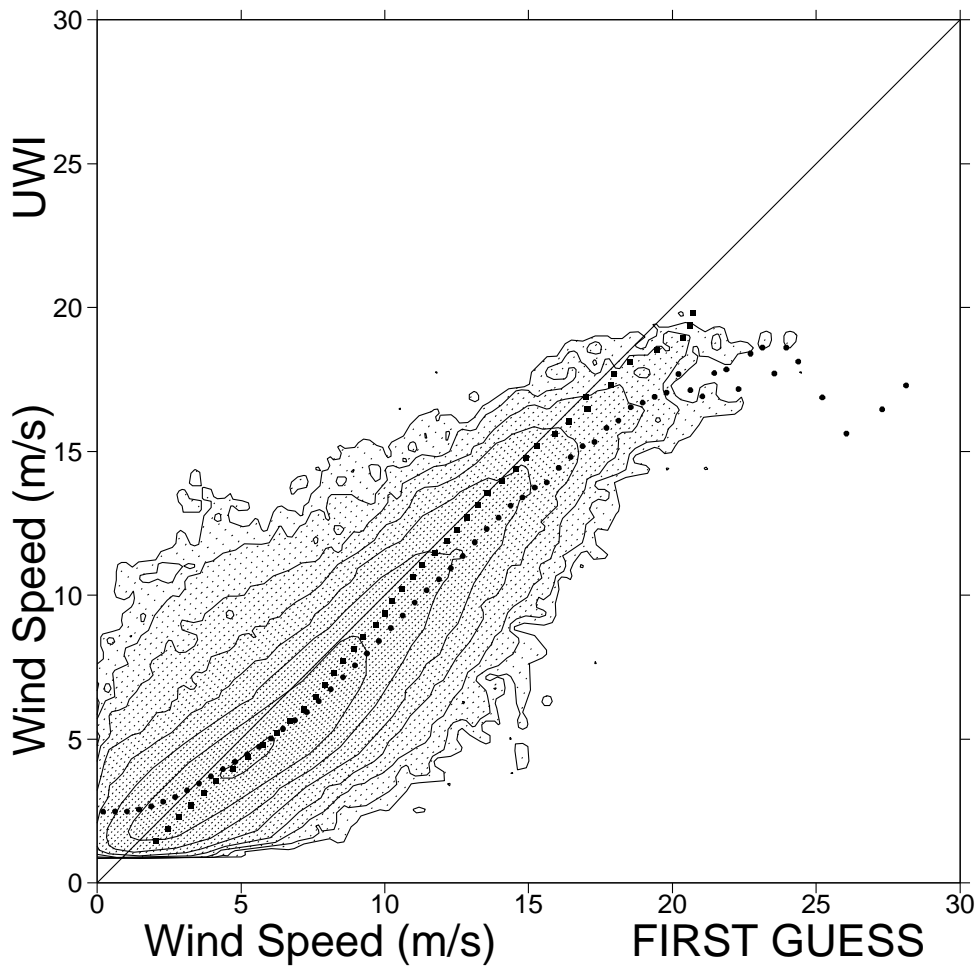


Figure 15

histogram of first guess 10 m winds versus uwi winds  
from 2004051800 to 2004030818  
= 606576, db contour levels, 5 db step, 1st level at 2.8 db  
 $m(y-x) = -0.35$   $sd(y-x) = 1.39$   $sdx = 2.96$   $sd y = 2.86$   $pcxy = 0.942$

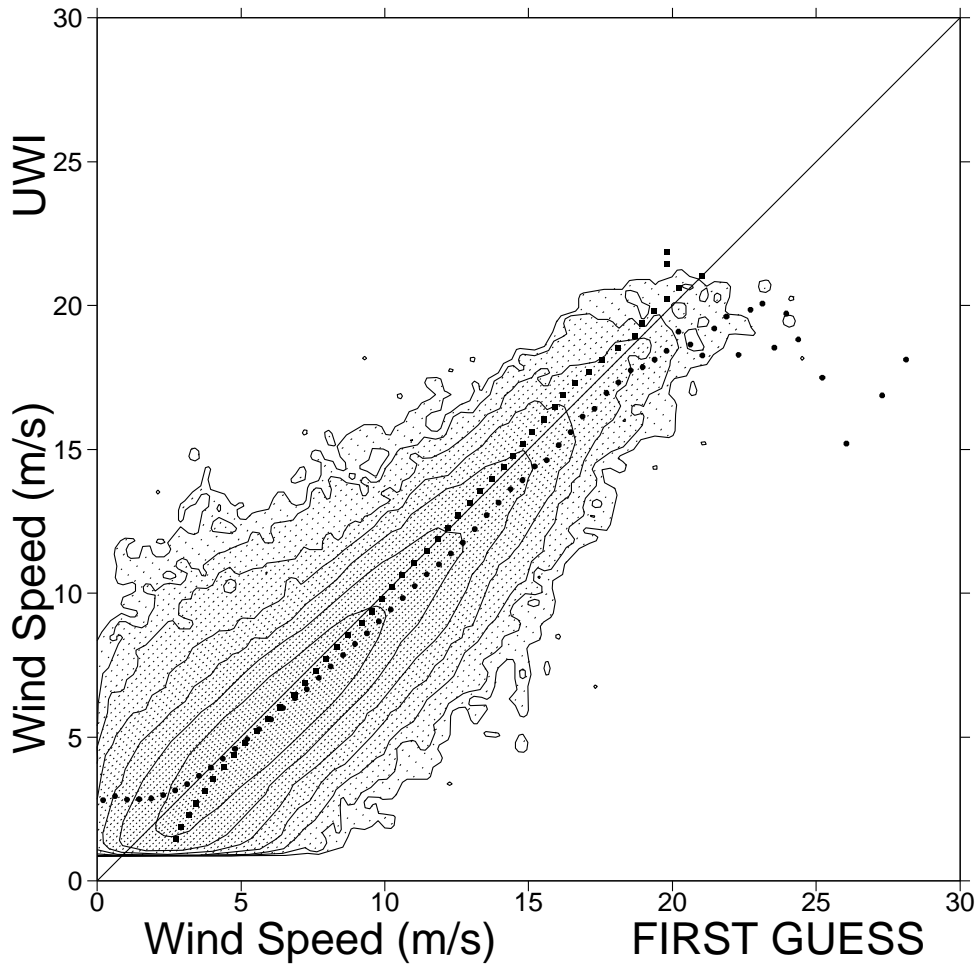
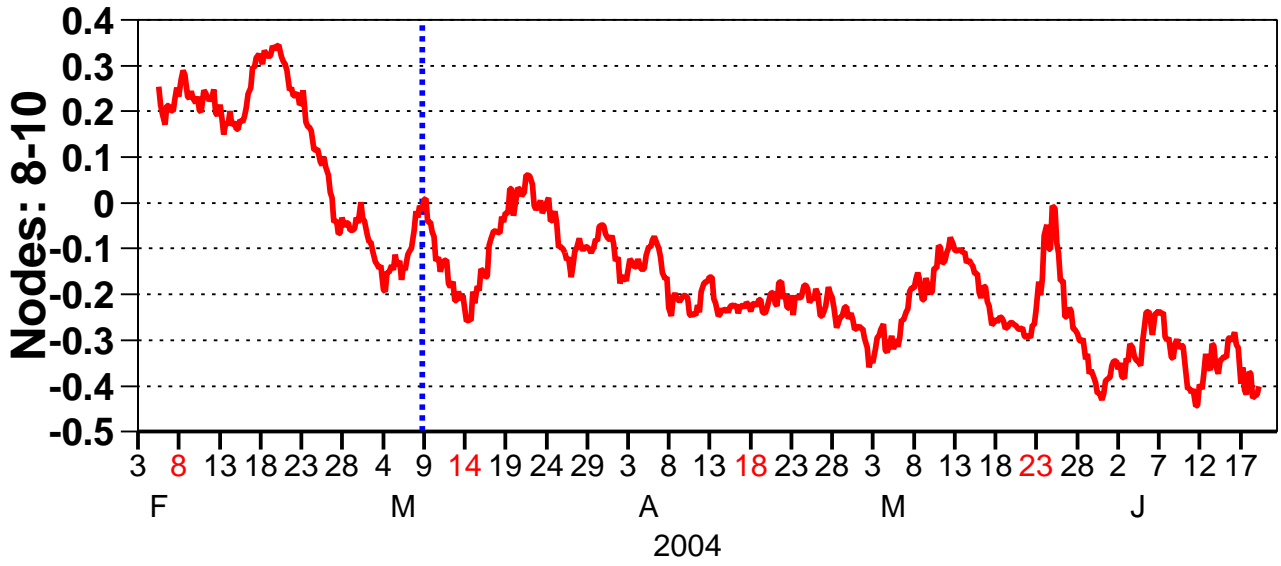


Figure 16

# ERS-2 (EC-CMOD4, CMOD5)



# QuikSCAT (QSCAT-1)

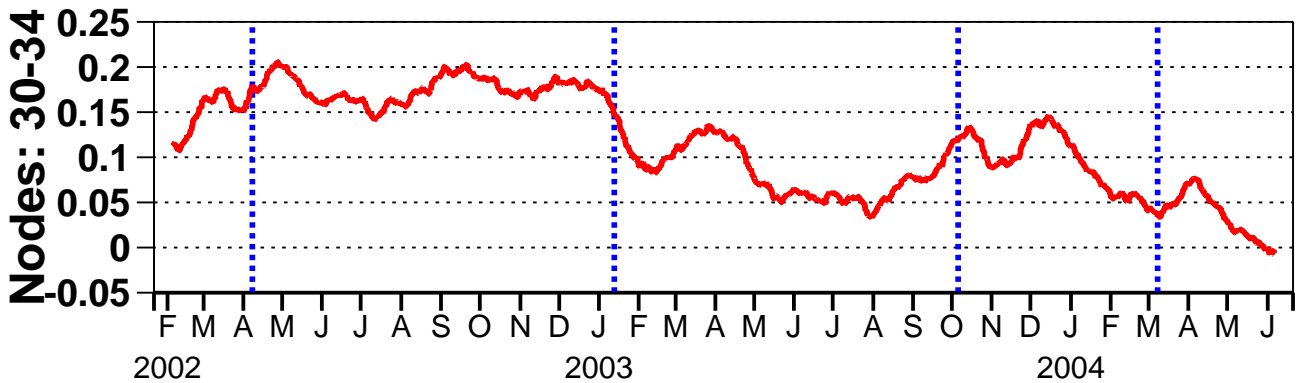
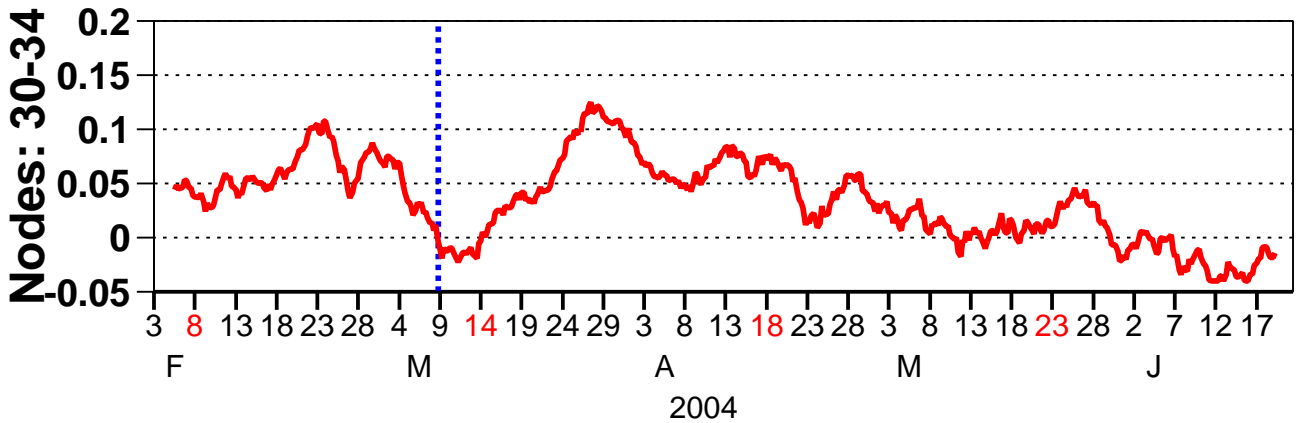


Figure 17